Astron. Astrophys. 354, 480–496 (2000)

ASTRONOMY AND ASTROPHYSICS

On the FIR emission from intracluster dust

Cristina C. Popescu[1,2], Richard J. Tuffs[1], Jörg Fischera[1], and Heinrich Völk[1]

[1] Max-Planck-Institut für Kernphysik, Saupfercheckweg 1, 69117 Heidelberg, Germany
[2] The Astronomical Institute of the Romanian Academy, Str. Cuţitul de Argint 5, 75212 Bucharest, Romania

Received 26 August 1999 / Accepted 22 November 1999

Abstract. We make predictions for the diffuse far-infrared (FIR) emission from dust in the intracluster medium (ICM) of the Virgo cluster using detailed information on potential dust sources, grain heating and sputtering rates available for this cluster from recent optical and X-ray studies. In the cluster core we identify the winds of red giant and supergiant IC stars as the main continuous sources of IC grains, with a dust injection rate of $0.17\,M_{\odot}yr^{-1}$. The predicted FIR surface brightness from this dust component is however a factor of ~ 10 below the detection limit of currently available telescopes. Grains that are impulsively removed from spiral galaxies by ram-pressure stripping as they enter the cluster core region can sporadically dominate the grain injection rate into the ICM. However, these events should lead to the appearance of rare, relatively bright, localised FIR sources around the parent galaxy.

The outer regions of dynamically young clusters like the Virgo cluster have a further potential source of intracluster grains since they are still accreting freshly infalling spiral galaxies which are presumably contained in an accreting intergalactic medium (IGM). We show that cosmics ray driven winds from the infalling spirals can inject grains into a subvirial IGM that is external to the observed X-ray-emitting ICM. Sputtering during the injection process and in the IGM is weak, so that the injected grains should accumulate in the IGM until the infall brings them into contact with the hot ICM. Normalising the mass loss rate in the galactic winds to the mass-loss rate and B-band luminosity of the Milky Way, we estimate a dust accretion rate of $1.0\,M_{\odot}yr^{-1}$ from the infalling IGM. This effect dominates the dust injection rate from known sources embedded in the hot Virgo ICM. Thus, any detection of diffuse IR emission would probe the current dust accretion rate for the cluster, acting as an indicator of the youth and the dynamical state of the cluster. The predictions for the Virgo cluster are generalised to other clusters and the possibility of detection of dynamically young clusters at cosmological distances is discussed. Although dominated by the discrete source emission from galactic disks, it is possible that diffuse sub-mm dust emission from the ICM could be detected in experiments similar to those designed to map the sub-mm excess due to the Sunyaev-Zeldovich effect in distant clusters.

Send offprint requests to: Cristina C. Popescu (popescu@levi.mpi-hd.mpg.de)

Key words: galaxies: clusters: individual: Virgo – galaxies: clusters: general – galaxies: intergalactic medium – galaxies: spiral – infrared: general – infrared: galaxies

1. Introduction

Hot gas in clusters can potentially be primordial in origin, heated adiabatically during the infall into the potential well, or it could alternatively be hot gas that was ejected from galaxies into the intracluster (IC) medium. Studies of X-ray line emission have revealed surprisingly high metallicities (0.4-0.5), suggesting that non-negligible or even a substantial fraction of the intracluster medium originated in galaxies. It has also been suggested that the ejected material could contain dust and that this dust could produce detectable FIR emission (Dwek et al. 1990). However, in the hot X-ray emitting plasma from the centre regions of clusters of galaxies the dust is quite efficiently sputtered and destroyed, on time scales of typically a few times 10^8 yr. To produce a detectable infrared emission this dust has to be injected at a high rate at the present epoch. Several indirect estimates indicating the presence of a substantial amount of grains in the IC medium, sufficient to detect in emission in the infrared, have been made. These have been derived from extinction measurements (Zwicky 1962; Karachentsev & Lipovetskii 1969; Bogart & Wagoner 1973; Boyle et al. 1988; Romani & Maoz 1992), from the soft X-ray absorption measurements (Voit & Donahue 1995, Arnaud & Mushotzky 1998) or from the observed amount of gas, by assuming that all the gas has been continuously injected with the Galactic gas-to-dust ratio, $Z_d = 0.0075$ since formation of the cluster (Dwek et al. 1990). However, it is not clear whether the current populations of elliptical and spiral galaxies seen in clusters are capable of supporting the required injection rate to achieve detectability of IR emission from the IC medium, or whether other sources might be required.

Observational evidence for FIR emission associated with intracluster dust has generally been inconclusive (Wise et al. 1993). Recently Stickel et al. (1998) detected a colour excess in the central 0.2 Mpc radius of Coma cluster, from the FIR emission measured by the ISOPHOT C200 camera aboard ISO. This colour excess was interpreted as thermal emission from intracluster dust with a temperature slightly higher than in the galactic cirrus and in cluster galaxies. However Quillen et al.

(1999) have argued that the measurement by Stickel et al. comes from cluster galaxies. They estimated that the galaxies in the central region of the Coma cluster would produce a surface brightness of 0.06 MJy/sr, which they take as being in agreement with the Stickel detection. Nevertheless, the Stickel et al. measurement represents only a lower limit and it was obtained after subtracting the contribution of foreground galactic cirrus and cluster galaxies, on the assumption that the latter emission would arise from cooler dust. In summary there are major theoretical and observational uncertainties concerning both the amount and source(s) of IC dust.

Here we make predictions for intracluster dust emission taking into account a variety of potential sources of dust. We illustrate the calculations using data for the Virgo Cluster, which is close enough for any intracluster IR emission to be spatially distinguished from emission from constituent galaxies and has detailed X-ray information, allowing realistic calculations of grain heating and sputtering time scales to be made. Furthermore, there is detailed information on all the Virgo galaxy members (Binggeli et al. 1993), and there has even been a recent detection of an intergalactic star population (Ferguson et al. 1998), which can be considered as a further potential source of intracluster grains. Finally, the Virgo cluster is the best studied example of a dynamically young cluster, into which spiral galaxies are falling in from the field (Tully & Shaya 1984). This allows a hitherto unconsidered, but potentially dominant, source of IC grains to be addressed, namely grains embedded in an external subvirial intergalactic (IG) medium accreting onto the X-ray emitting intracluster medium.

The plan of this paper is as follows: In Sect. 2 we give details of the calculation of the infrared emission from stochastically heated grains in the Virgo IC medium, for grain populations arising from a balance between steady state injection and sputtering. In Sect. 3 we estimate the dust injection rate from potential sources (elliptical and spiral galaxies and IC stars) currently seen in the core of the Virgo cluster. We show that these sources are unlikely to provide enough dust to be detected in the IC medium by current infrared observatories. In Sect. 4 the feasibility of accretion of grains injected into an external intergalactic medium from distant infalling spiral galaxies is discussed. For plausible subvirial gas inflows and physical conditions in the intergalactic medium it is concluded that once grains have been injected into the intergalactic medium, they will descend largely unmodified into the cluster, approximately comoving with the infalling IG medium, and accumulate over the infall timescale. In Sect. 5 we make detailed estimates for the efficiency of the grain injection into the IG medium by calculating grain sputtering in outflow models for quiescent and star-burst galaxies. We find that dust grains can survive in winds from quiescent (non-starburst) galaxies and that their size distribution is not significantly changed by sputtering. In Sect. 6 we estimate the grain accretion rate from the B-band luminosity of the infalling population of spiral galaxies, finding this to be the main source of grains entering the IC medium. Once the grains reach the hot IC medium they radiate in the infrared and are sputtered on timescales smaller than the infall timescale. Calculations of the spectrum of the IR/submillimeter radiation of the accreted grains are given both for grains in the outer regions of the diffuse X-ray plateau, and for grains directly brought into contact with the dense core region. Some implications of the results are discussed in Sect. 7. A distance of 18.2 Mpc to the Virgo cluster is assumed throughout.

2. Calculation of the infrared emission

In low-density hot astrophysical plasmas a dust particle is predominantly heated stochastically by the ambient gas and undergoes temperature fluctuations (Gail & Sedlmayr 1975, Draine & Anderson 1985, Dwek 1986, Dwek & Arendt 1992). To calculate the temperature distribution for different grain sizes in the cluster we adopted the parameters of the IC gas from Böhringer et al. (1994), Nulsen & Böhringer (1995) and Schindler et al. (1999) based on ROSAT observations. The X-ray morphology of the cluster was found to be very similar to the structure in the galaxy distribution, with a major component around M87 and a smaller component around M49. A faint diffuse component was also found to trace the cluster out to a distance of $4-5^{\circ}$ from M87 (also seen by the Ginga satellite; Takano et al. 1989). The diffuse emission is rather asymmetric, falling off more steeply to the western side of the cluster. Because of the irregular structure, previous authors have divided the inner regions of the cluster into separate spherically symmetrical components centred on M87, M86 and M49, modelling the X-ray emission of each assuming hydrostatic equilibrium. Thus 71% of the total X-ray luminosity originates from the M87 halo (out to 1° from M87) and 15% comes from the diffuse X-ray component extending to $4-5^{\circ}$ from M87.

To calculate grain heating and sputtering rates within the cluster core we adopt the deprojected radial density and temperature profiles of Nulsen & Böhringer (1995), who divided the inner part of the cluster into 38 concentric spherical shells. Their results are reproduced in Table 1 (where we have binned together shells for which the temperature is constant). The abundances were fixed at 0.45 solar (Koyama et al. 1991; referred to Cosmic values in Allen 1973). Some recent results based on ASCA observations (Matsumoto et al. 1996) indicate a higher temperature for the hot plasma in the inner $10'$ of the cluster. However, as no deprojected model is yet available for the new ASCA data, we will use the ROSAT results throughout this paper.

To calculate grain heating and sputtering rates appropriate for grains injected at the perimeter of the diffuse intracluster medium we estimated the plasma density at a distance of $4-5^{\circ}$ from M87 using the results of Böhringer et al. (1994). These authors quote the total spatially integrated flux of the diffuse component as seen by ROSAT to be 15% of the total X-ray flux. Assuming spherical symmetry and the broad band emissivity being bremsstrahlung dominated, the corresponding average gas density is given by:

$$n_1^2 = \frac{F_1}{F_2}\,\frac{\sum n_i^2\,V_i\,T_i^{1/2}}{V_1\,T_1^{1/2}} \qquad (1)$$

Table 1. Density and temperature distribution of hot gas in the core of Virgo Cluster

radius ($'$)	n_e (cm^{-3})	T_e (K)
0.00-1.67	0.0358	1.30×10^7
1.67-3.33	0.0149	1.61×10^7
3.33-5.00	0.0092	2.70×10^7
5.00-6.67	0.0065	2.00×10^7
6.67-7.50	0.0058	1.69×10^7
7.50-9.17	0.0049	2.36×10^7
9.17-11.25	0.0039	2.67×10^7
11.25-13.75	0.0029	3.13×10^7
13.75-16.25	0.0023	2.38×10^7
16.25-21.25	0.0019	3.13×10^7
21.25-26.67	0.0012	1.35×10^8
26.67-37.08	0.0008	3.71×10^7
37.08-51.25	0.0007	3.37×10^7

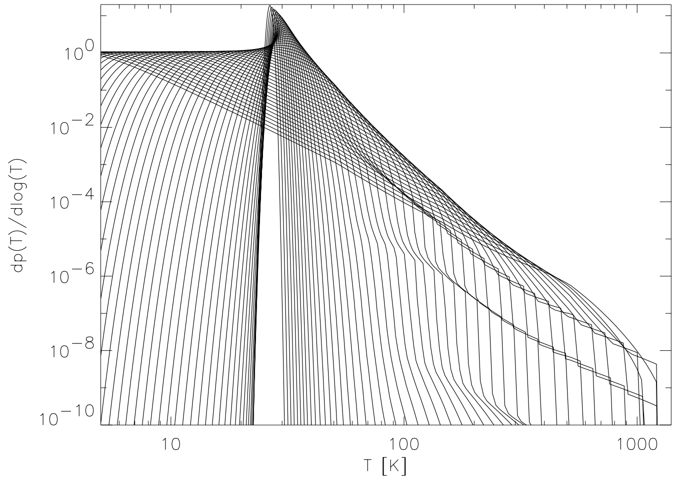

Fig. 1. The temperature distribution for various silicate grain sizes in the centre region of $1'.67$ radius of the Virgo Cluster. The grain sizes are chosen in the size interval from 10 Å to 0.25 μm, with a logarithmic step size of 0.05. The electron density and temperature in this region are given in Table 1.

where n_1, V_1, F_1 and T_1 are the density, volume, flux and temperature of the diffuse X-ray component of the cluster and n_i, V_i, F_i and T_i are the same quantities, associated with the spherical shells within the halo of M87 (see Table 1). Since the temperature remains constant outside the halo of M87 with a temperature of $\sim 3 \times 10^7$ K (Böhringer et al. 1994), we obtain an average gas density for the diffuse component of $4 \times 10^{-5}\,\mathrm{cm}^{-3}$. This is comparable with the gas density at the edge of the diffuse emission region which can be derived from Schindler et al. (1999), for a model where the gas is in hydrostatic equilibrium.

In the hot intracluster medium the grains are heated due to inelastic collisions with electrons and ions. In characterising the dust properties we considered spherical "astronomical silicate" grains and heat capacities from Guhathakurta & Draine (1989), derived as a fit to experimental results for SiO_2 and obsidian at temperatures $10 < \mathrm{T} < 300\,\mathrm{K}$ (Leger et al. 1985), with a simple extrapolation for $\mathrm{T} > 300\,\mathrm{K}$. In Sect. 6 we also considered graphite grains, with heat capacities taken from Dwek (1986). The absorption efficiencies Q_ν(a) were taken from Laor & Draine (1993) with grain sizes in the size interval $[a_{min}, a_{max}]$ from 10 Å to 0.25 μm.

For the heating of the grains in a hot plasma we adopted the method used by Dwek (1987). Here the grain is assumed to have an effective thickness $R_0 = 4a/3$ and let R(E) be the range at which gas particles with kinetic energy E would be stopped. If R(E) is shorter than the effective thickness, then all energy will go onto the grain. Otherwise the gas particles will have a rest energy E', that is given by $R(E') = R(E) - R_0$.

In the case of electron heating we used an analytical expression of the electron stopping power R(E)ρ for silicate and graphite from Dwek & Smith (1996). In the case of ion heating the energy fraction deposited by ions onto the grains was calculated with a formula similar to that used by Dwek & Werner (1981), which is based on an approximation from Draine & Salpeter (1979), for the range of H and He in solids up to 100 keV:

$$\zeta(\mathrm{E}) = \begin{cases} 1 & , \quad \mathrm{E} < \mathrm{E}^*, \\ \mathrm{E}^*/\mathrm{E} & , \quad \text{otherwise}, \end{cases} \tag{2}$$

where E^* is the minimum kinetic energy of a nucleus to penetrate the grain. It is given by

$$\mathrm{E}^*[\mathrm{keV}] = \frac{1}{3}\, \mathrm{a}[\mu m]\, \rho[\mathrm{g/cm^3}] \times \begin{cases} 133 & \text{for H atoms}, \\ 222 & \text{for He atoms}, \\ 665 & \text{for C, N, O atoms}. \end{cases} \tag{3}$$

This shows that in a hot gas the ion heating of very small grains is nearly discrete.

In low density plasma, like that existing in the intracluster medium, the grains are mainly stochastically heated. The stochastic heating processes are calculated following the method of Guhathakurta & Draine (1989). This method derives the temperature distribution P(a,T_d) of various grain radii **a** as a function of dust temperature T_d.

In Fig. 1 we give the temperature distribution P(a,T_d) for various silicate grain sizes, for the inner $1'.67$ radius of the Virgo Cluster ($n_e = 0.0358\,\mathrm{cm}^{-3}$, $T_e = 1.30 \times 10^7$). Due to stochastic heating, small grains undergo significant fluctuations from the equilibrium temperature, while larger grains have probability functions becoming narrower, eventually approaching delta functions. Many of the smaller grains exhibit a plateau in their probability distribution, separated by steps corresponding to the energy thresholds at which the various ions are stopped by the grains (see Eqs. (2) and (3)).

In order to calculate the contribution of all grain sizes we have to derive the grain size distribution. We consider that the grains are continuously injected in the IC medium with a grain size distribution given by a power law, a^{-k}. The mechanism through which they can be injected is discussed in the next sections; here we consider the general case. The grain size distribution can be determined approximately by balancing the local rate of grain injection into the ICM, S(a), and the rate of grain destruction by sputtering:

$$\frac{\partial}{\partial \mathrm{a}} \left(\mathrm{N(a)} \, \frac{\mathrm{da}}{\mathrm{dt}} \right) = \mathrm{S(a)} \tag{4}$$

where N(a) da is the total number of particles with sizes in the interval [a,a+da].

For gas temperatures $10^6 < \mathrm{T} < 10^9\,\mathrm{K}$ the sputtering timescale for a silicate or graphite dust particle of radius a is given by Draine & Salpeter (1979):

$$\mathrm{t_{sput}[yr]} \approx \frac{10^6\,\mathrm{a}[\mu\mathrm{m}]}{\mathrm{n_H[cm^{-3}]}} \tag{5}$$

where $\mathrm{n_H}$ is the gas density.

From Eqs. (4) and (5) results the steady state grain size distribution:

$$\mathrm{N(a)} = \frac{\mathrm{t_{sput}}}{\mathrm{a}} \, \frac{\mathrm{dM_i}}{\mathrm{dt}} \, \frac{\mathrm{a}^{-k+1} - \mathrm{a}_{\mathrm{max}}^{-k+1}}{\mathrm{k}-1} \times \times \left[\int_{a_{\mathrm{min}}}^{a_{\mathrm{max}}} \mathrm{a}^{-k} \, \frac{4\,\pi\,\mathrm{a}^3}{3} \, \rho \, \mathrm{da} \right]^{-1} \tag{6}$$

where ρ is the density of the dust grains and $\mathrm{dM_i/dt}$ is the total dust injection rate:

$$\frac{\mathrm{dM_i}}{\mathrm{dt}} = \int_{a_{\mathrm{min}}}^{a_{\mathrm{max}}} \mathrm{S(a)} \, \frac{4\,\pi\,\mathrm{a}^3}{3} \, \rho \, \mathrm{da} \tag{7}$$

The total dust mass is then given by:

$$\mathrm{M} = \int_{a_{\mathrm{min}}}^{a_{\mathrm{max}}} \mathrm{N(a)} \, \frac{4\,\pi\,\mathrm{a}^3}{3} \, \rho \, \mathrm{da} \tag{8}$$

and the total infrared emission is:

$$\mathrm{F}_\nu \;=\; \frac{1}{\mathrm{d}^2} \int_{a_{\mathrm{min}}}^{a_{\mathrm{max}}} \mathrm{N(a)\,da}\,\pi\,\mathrm{a}^2\,\mathrm{Q}_\nu(\mathrm{a}) \times \times \int_0^\infty \mathrm{B}_\nu(\mathrm{T_d})\,\mathrm{P(a,T_d)}\,\mathrm{dT_d} \tag{9}$$

where B_ν is the Planck function.

3. Predicted FIR emission from intracluster dust produced by sources inside the core region of the Virgo cluster (within 1° of M87)

3.1. Dust originating in individual intergalactic stars

In this section we estimate the amount of dust produced through stellar winds by individual intergalactic red-giant-branch stars, as detected recently in the Virgo cluster by Ferguson et al. (1998). The motivation to consider these stars as potential sources of dust was the suggestion that the intergalactic stars are likely to have originated primarily from the elliptical and S0 galaxies, and thus to contain a higher proportion of M supergiants to giants as compared to the Galactic disk, and therefore a higher integrated mass-loss and dust production. Furthermore, this dust would not suffer sputtering losses in the injection process, as is the case for injection from galaxies into the intracluster medium through galactic winds. According to Ferguson et al. the relatively smooth distribution of mass inferred from the X-ray observations suggests that most of the intergalactic material was stripped by tidal interactions with the cluster potential. Since early-type galaxies are more numerous in the cluster, have older stellar populations, and are likely to have inhabited the central megaparsec of the cluster for much longer than the spiral and irregular galaxies, we will consider here that the intergalactic stars were stripped from early type galaxies. Nevertheless, the possibility that some of the stars formed in situ, or that some were stripped off by impulsive interactions between galaxies (‘harassment’, Moore et al. 1996) cannot be ruled out (Ferguson et al. 1998).

The observations made with the Hubble Space Telescope WFPC2 camera with the F814W (approximately I-band) filter on a blank field in the Virgo cluster (Ferguson et al. 1998) indicated a clear excess in source counts in the Virgo cluster image. The total flux from the excess sources was used by Ferguson et al. to calculate the total mass of stars below their detection limits. For this they considered a population with a metallicity, expressed as a decimal logarithm relative to the solar iron-to-hydrogen ratio, [Fe/H]=-0.7, an age of 13 Gyr, a Salpeter initial mass function, and a distance of 18.2 Mpc. They derived an underlying surface mass density of 0.14 $\mathrm{M_\odot\,pc^{-2}}$ if the initial mass function continues to 0.1 $\mathrm{M_\odot}$.

To calculate the total mass loss of all the stars within the X-ray emitting core region of 60 arcmin radius from the position of M87, we consider that the stars follow the distribution of elliptical (E) and S0 galaxies. Their distribution is described by a spherical King model:

$$\rho(\xi) = \rho_0\,(1+\xi^2)^{-3/2} \tag{10}$$

where ρ_0 is the central mass density of stars, $\xi = \mathrm{r/r_c}$ is the radius in units of the core radius $\mathrm{r_c}$. We take the core radius $\mathrm{r_c} = 1.1°$, as given for the E+S0 Virgo galaxies by Binggeli et al. (1987). The projected mass surface density of stars is then:

$$\Sigma(\lambda) = \frac{2\,\rho_0\,\mathrm{r_c}}{(1+\lambda^2)} \left(1 - \frac{1+\lambda^2}{1+\xi_\mathrm{t}^2}\right)^{1/2} \tag{11}$$

where $\lambda = \mathrm{R/r_c}$ is the projected radius in units of the core radius and $\xi_\mathrm{t} = \mathrm{r_t/r_c}$ is the radius of the outer boundary in units of core radius. If we consider a surface mass density of intracluster stars of 0.14 $\mathrm{M_\odot\,pc^{-2}}$, as derived by Ferguson et al. (1998) at a distance of 44.5 arcmin from M87, from Eq. (10) we obtain the central mass density of stars, $\rho_0 = 0.363 \times 10^{-6}\,\mathrm{M_\odot\,pc^{-3}}$.

The stellar mass within radius ξ in units of the stellar core mass $\mathrm{M_c}$ is:

$$\mathrm{M}(\xi) = 3[\ln(\xi + (1+\xi^2)^{1/2}) - \xi(1+\xi^2)^{-1/2}] \tag{12}$$

with the core mass

$$\mathrm{M_c} = \frac{4\,\pi\,\mathrm{r_c^3}\,\rho_0}{3} \tag{13}$$

Table 2. The distribution of stellar masses and dust injection rates in the central region of the Virgo cluster.

1 r (′)	2 M_{stars} ($M_\odot$)	3 $\dot{M}_i$ ($M_\odot\,yr^{-1}$)
1.67	1.05e+06	4.96e-06
3.33	7.26e+06	3.93e-05
5.00	1.98e+07	1.33e-04
6.67	3.83e+07	3.14e-04
7.50	2.78e+07	4.45e-04
9.17	7.69e+07	8.08e-04
11.25	1.42e+08	1.48e-03
13.75	2.51e+08	2.66e-03
16.25	3.54e+08	4.34e-03
21.25	1.06e+09	9.34e-03
26.67	1.75e+09	1.76e-02
37.08	5.23e+09	4.23e-02
51.25	1.07e+10	9.29e-02
Total	2.0e+10	0.17

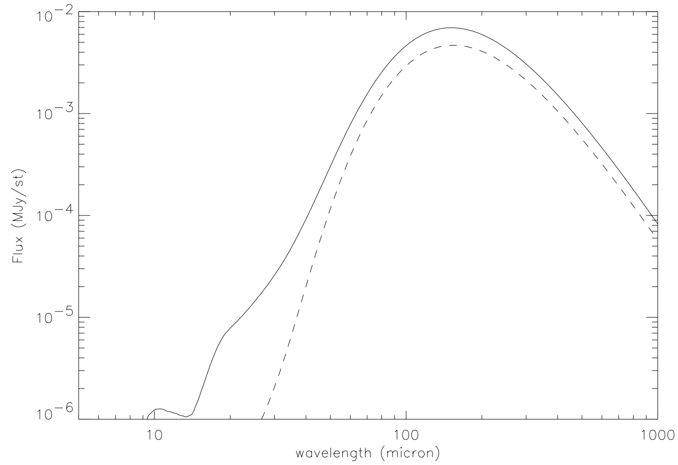

Fig. 2. The integrated line-of-sight spectrum in the centre of Virgo cluster, given for different sources of dust inside the X-ray emitting core region: solid line for stars and dashed-line for elliptical galaxies. A silicate dust composition was assumed.

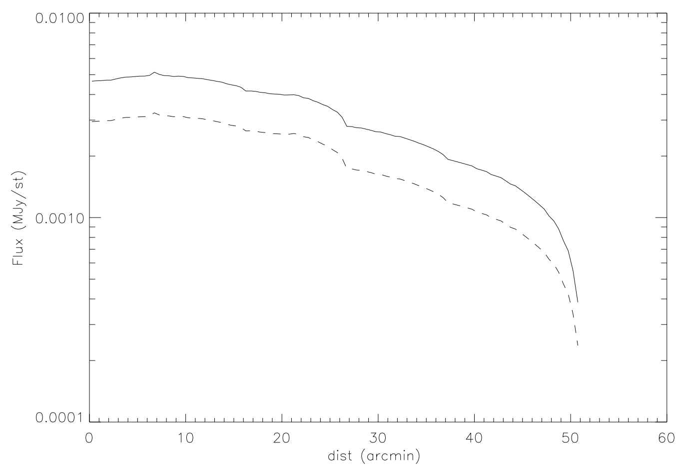

Fig. 3. The infrared brightness profile at 100 μm for different sources of dust inside the X-ray emitting core region: solid line for stars and dashed-line for elliptical galaxies. A silicate dust composition was assumed.

From Eqs. (10) and (11) we calculate the stellar mass in each of the spherical shells from Table 1 and the results are given in Table 2, Column 2. In order to obtain the number of stars of different spectral types and luminosity classes that correspond to the derived total mass we have to integrate over the mass function of such a population. We consider a model HRD population for an elliptical galaxy assuming the same parameters as used by Ferguson et al. (1998) to derive the total mass of the stars. For the mass-loss rates and gas to dust ratio in the outflow of different types of stars we took the values from Whittet (1992) and Gehrz (1989) for the Galactic stellar population. Whilst bearing in mind that the averaged mass-loss and dust to gas ratio are subject to considerable uncertainty, we may draw some general conclusions from these data. Summing individual injection rates for stardust we obtain a total injection rate of dust $\dot{M}_i$ for each spherical shell, and the corresponding values are given in Table 2, Column 3. The main contribution to the injection rate comes from M supergiants, which would imply that most of the grains should consist of silicates.

The values of the dust injection rate are quite low, indicating that there are not enough stars to produce a detectable amount of dust in the inner hot region of the cluster, since the grains are sputtered very efficiently by the ambient hot gas.

We assume that the grain size distribution injected into the IC medium by the stars is given by a power law with an exponent given by the MRN (Mathis et al. 1977) value of k=3.5. We also assume a silicate dust composition. From Eqs. (8) and (9) we calculated the infrared intensity at different projected distances from the cluster by integrating over the line of sight through the cluster. The corresponding infrared spectrum in the inner $1'.67$ region of the Virgo cluster is plotted with a solid line in Fig. 2, while in Fig. 3 we give the radial brightness profile at 100 μm. The infrared emission from dust injected by intergalactic stars inside the core region of the Virgo cluster is less than 0.01 MJy/st, about an order of magnitude below the detection limit of ~ 0.1 MJy/st for currently available telescopes.

3.2. Dust originating in early type galaxies

The elliptical and S0 galaxies are not only the best candidates for the sources of the intracluster stars (discussed in the previous section), but they are also thought to release gas into the ICM via supernovae-driven galactic winds. Because these galaxies have remained in the inner region of the cluster since their formation, their integrated mass-loss has been used (Okazaki et al. 1993) to calculate the galaxian contribution to the observed amount of gas in the centre of the cluster. Okazaki et al. selected all E, S0 and dwarf elliptical galaxies from the Virgo Cluster Catalogue of Binggeli et al. (1985), in the field within 3° from M87. They used three models for elliptical galaxy formation with galactic

Table 3. Upper limits for the distribution of dust injection rates produced by elliptical galaxies in the central region of the Virgo cluster.

1	2
r	$\dot{M}_i$
($'$)	($M_\odot$ yr^{-1})
1.67	1.19e-06
3.33	9.46e-06
5.00	3.20e-05
6.67	7.56e-05
7.50	1.07e-04
9.17	1.95e-04
11.25	3.57e-04
13.75	6.43e-04
16.25	1.05e-03
21.25	2.26e-03
26.67	4.25e-03
37.08	1.02e-02
51.25	2.24e-02
Total	4.15e-02

winds (Arimoto & Yoshii 1987, Matteucci & Tornambe 1987, David et al. 1990,1991a,b) and estimated the masses of gas that have been ejected from all these galaxies during the cluster lifetime. The result was that even the largest mass obtained by one of their model prediction is only 10% of the value derived from X-ray observations. They concluded that elliptical galaxies cannot produce the observed amount of gas and that 90% of the gas must be of primordial origin. In the case of the dust released by elliptical galaxies via supernovae-driven galactic winds, it is obvious that only the dust produced quite recently can give rise to an IR emission, since the dust is quickly sputtered away. But elliptical galaxies have released most of their gas in the earlier epochs of the cluster lifetime, so their current injection rate is low. We will show that even for the most optimistic assumption, of a steady state mass-loss over the cluster lifetime, only a negligible amount of dust is predicted, since the elliptical galaxies are well depleted of dust in comparison with the spiral galaxies (Tsai & Mathews 1996). Thus if we take the amount of gas predicted by Okazaki et al., an average dust-to-gas ratio a hundred times lower than the Galactic value (Tsai & Mathews 1996) and if we divide this value by the cluster lifetime we obtain an average dust injection rate which is an upper limit for the present dust injection rate. Tsai & Mathews (1995) have shown that in the elliptical galaxies the grain size distribution is given by a power law with index $(k-1)$. They have also shown that this solution is valid when the sputtering time is short compared to the radial flow time, but the same solution is still an excellent approximation even when the sputtering time is so long that the grains can move inwards during their lifetime across an appreciable part of the galaxy. Assuming again that the grains in the elliptical galaxies are injected from the evolving stars with a power law having the MRN index $k = 3.5$, the size distribution of the ellipticals will be a power law of index 2.5. We also assume that the grain size distribution is not modified inside the galactic wind and that the dust consists of silicate grains. With these assumptions we calculated the dust injection rate in the same spherical model for the cluster core as previously used (Table 1). The results are given in Table 3.

The corresponding spectrum and brightness profile at 100 μm are given in Figs. 2 and 3 with dashed lines. The amount of infrared emission produced by dust ejected by all early type galaxies in the inner core of Virgo cluster is negligible even in the upper limit calculation, being only at best comparable to the emission from stellar dust.

3.3. Dust originating in late-type galaxies

Late-type galaxies are known to contain more dust than the elliptical galaxies, and they can eject interstellar gas through interaction with the cluster environment. Haynes & Giovanelli (1986) have shown that Virgo spirals within 5 degrees of M87 are HI deficient compared with their field counterparts. The HI deficiency becomes more marked for the central regions, with three-quarters of Virgo spirals within 2.5 degrees of M87 deficient by more than a factor 3 ($\mathrm{DEF} > +0.47$). The summation of HI deficiency by gas mass for spirals seen in projection within 5 degrees of M87 (as tabulated by Giovanelli & Haynes 1983 and Haynes & Giovanelli 1986) is $5.7\times10^{10}\,M_\odot$, with the bulk of the summed deficiency being due to the giant spirals. Taking the dust (and gas) replenishment timescale in galactic disks to be comparable to that estimated for the Milky Way of $\sim 3\times10^9$yr (e.g. Jones et al. 1997) one can estimate a current gas injection rate of $\sim 19\,M_\odot yr^{-1}$ into the Virgo ICM from spiral galaxies. The dust content of the diffuse HI prior to ejection is difficult to estimate. On the one hand gas is preferentially lost from the outer disk, where the metallicity and dust abundance is typically lower than that for the galaxy as a whole. On the other hand, it is known that spirals in the Virgo core have an enhanced metallicity by a factor of approximately 2 compared with field counterparts of similar lateness (Skillman et al. 1996). Assuming that the ejected gas originally contained dust with an abundance of 0.0075 by mass (i.e. that of the Milky Way), we obtain a crude upper limit for the dust injection rate into the Virgo ICM of $0.14\,M_\odot yr^{-1}$. This upper limit corresponds to the case that grain sputtering in the injection process from the interstellar to the intracluster medium can be ignored. It is somewhat lower that the estimated injection rate from the intracluster star population.

Whether the actual dust injection from spirals into the IC medium approaches this upper limit is likely to depend on the mechanism for ejection. The most favoured model for gas removal from the HI deficient galaxies, as originally proposed by Gunn & Gott (1972), is ram-pressure stripping, whereby gas can be removed if the ram pressure $P_{ram} \sim \rho_{ICM}\, v_{gal}^2$ exceeds the gravitational restoring force per unit area on the diffuse HI gas, $P_{grav} = 2\pi\, G\, \sigma_{grav}\sigma_{HI}$. Here v_{gal} is the relative velocity of the galaxy through the IC medium of density ρ_{ICM}, and σ_{grav}, σ_{HI} are the gravitational and HI gas surface densities in the galactic disk, respectively. Typically, giant spirals have $\sigma_{HI} \sim 10\,M_\odot pc^{-2}$ averaged over the disk (e.g. Roberts & Haynes 1994; Young & Scoville 1991); the

Milky Way has $\sigma_{\rm HI} \sim 5\,{\rm M_\odot pc^{-2}}$ at the solar circle (Dickey & Lockman 1990). Within 1° of M87, $\rho_{\rm ICM} \geq\sim 10^{-24}{\rm kg\,m^{-3}}$, and typically $v_{\rm gal} \sim 1000\,{\rm km\,s^{-1}}$. This is sufficient to strip diffuse interstellar HI with $\sigma_{\rm HI} \leq 10\,{\rm M_\odot pc^{-2}}$ from within a giant spiral like the Milky Way, which has (Bahcall et al. 1992) $\sigma_{\rm grav} \sim 70\,{\rm M_\odot pc^{-2}}$ at the solar circle. To estimate whether grains would be sputtered in this process we note that a sudden interaction of a galaxy with the IC medium would generally drive a shock wave into a cold diffuse HI disk of density $\rho_{\rm HI}$ with speed $v_{\rm s} \sim (\rho_{\rm ICM}/\rho_{\rm HI})^{0.5}\,v_{\rm gal}$. For mid-plane number densities of $\sim 0.5\,{\rm cm^{-3}}$, as in the diffuse HI in the plane of the Milky Way at the solar circle (Dickey & Lockman 1990), $v_{\rm s}$ is $37\,{\rm km\,s^{-1}}$, for $v_{\rm gal} \sim 1000\,{\rm km\,s^{-1}}$ and $\rho_{\rm ICM} \sim 10^{-24}{\rm kg\,m^{-3}}$ (i.e. 1° from M87). This shock speed is well below the minimum value of $\sim 100\,{\rm km\,s^{-1}}$ needed for sputtering. Although sputtering should become effective in ram-pressure stripping from the outer disk, where HI number densities may be orders of magnitude lower, this simple consideration is consistent with the possibility that a substantial fraction of the interstellar grains may survive the ram-pressure stripping process. Indeed, some direct evidence for the presence of dust in interstellar material stripped from the Virgo elliptical galaxy M84 has been found by Rangarajan et al. (1995).

High resolution hydrodynamical simulations of ram-pressure stripping of elliptical galaxies (Balsara et al. 1994) show that the gas removal involves a series of individual events separated by $\tau_{\rm strip}$ of a few times 10^{7} yr, leading to long tongues of stripped gas in the IC medium, a result which Balsara et al. consider would also apply to gas stripping from spirals. Once injected into the IC medium, the grains will be rapidly sputtered by the hot gas, so that the infrared emission should still be morphologically associated with the parent galaxy as a dust trail (Dwek et al. 1990), rather than being smoothly distributed in the IC medium. For the example of an ambient number density of $0.0007\,{\rm cm^{-3}}$ (corresponding to 1° from M87 - see Table 1), the sputtering time scale (Eq. (5)) is 1.4×10^{8} yr for grains of size $0.1\mu m$. The length of the infrared-emitting dust trail is then the distance traveled by the galaxy in this sputtering time, or 146 kpc for $v_{\rm gal} \sim 1000\,{\rm km\,s^{-1}}$.

We have estimated the infrared emission from a giant spiral with a radius of 20 kpc and an initial HI mass of about $6.6 \times 10^{9}\,{\rm M_\odot}$. For a typical HI deficiency (Haynes & Giovanelli 1986) of DEF=+0.47, the total HI mass loss is $4.4\times10^{9}{\rm M_\odot}$. Assuming most of the loss is sudden, on entering the cluster core region, and taking the dust-to-gas ratio to be $Z_{\rm d} = 0.0075$ (the Galactic value), then the mass of the dust released in the ICM medium by such a galaxy is $M_d = 3.3\times10^{7}\,{\rm M_\odot}$. The infrared spectrum of such a source is given in Fig. 4, for two cases; the first case (solid line) is when the stripping occurs at 10′ from the cluster centre, ($n_{\rm e} = 0.0039\,{\rm cm^{-3}}$, $T_{\rm e} = 2.36\times10^{7}$ K, see Table 1) and the second case (dashed-line) is when stripping occurs while the galaxy enters the dense core region of the cluster, at 1° distance from the centre of the cluster ($n_{\rm e} = 0.0007\,{\rm cm^{-3}}$, $T_{\rm e} = 3.37\times10^{7}$ K, see Table 1). It is interesting to note that the IR flux density of the transient IR emission from the dust trail is predicted to rival that of the photon-heated dust in the galactic disk, and, despite the difference in heating mechanism, have similar colours (with a spectral peak in the 100-200 μm range). This, combined with removal of dust from the disk, and hence reduced internal extinction, will create a discrete system with brighter apparent blue magnitudes and a boosted spatially integrated IR flux density. If seen in a distant cluster, where the intracluster IR component could not be resolved from the disk component, this could create the illusion of a galaxy with an enhanced star-formation activity, even though the star-formation in the galaxy may actually be somewhat suppressed by the gas removal in reality.

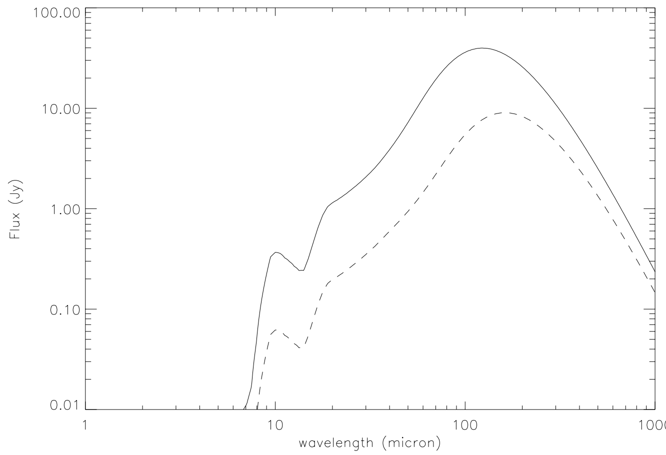

Fig. 4. The infrared spectrum of $M_{\rm d} = 3.3\times10^{7}\,{\rm M_\odot}$ of dust stripped from a spiral galaxy while infalling into the dense core region of the cluster. Solid line is when stripping occurs at 10′ from the cluster centre, ($n_{\rm e} = 0.0039\,{\rm cm^{-3}}$, $T_{\rm e} = 2.36\times10^{7}$ K, see Table 1) and dashed-line is when stripping occurs while the galaxy enters the dense core region of the cluster, at 1° distance from the centre of the cluster ($n_{\rm e} = 0.0007\,{\rm cm^{-3}}$, $T_{\rm e} = 3.37\times10^{7}$ K, see Table 1). A silicate dust composition was assumed.

Since spirals are more spread over the whole cluster area, following the density-morphological relation (Dressler 1980), they are by far less numerous in the centre of the Virgo cluster. From the number density profiles of late-type galaxies in the Virgo Cluster and assuming a King profile with a core radius $r_{\rm c} = 3.2°$ (Binggeli et al. 1987) we estimate only a few spirals (~ 2 galaxies) in the inner 1° from the cluster centre. As ram-pressure stripping is likely to be a transient phenomenon, occurring when the galaxies enter the dense core region of the IC medium, with sputtering timescales shorter than the time to traverse the angular extent of the core, we expect only of order 1 short-lived intracluster IR source in the inner 1° region of the cluster. To conclude, the IR emission coming from dust stripped from late-type galaxies is localised and connected to the parent galaxy, and does not account for a diffuse intracluster IR component.

4. An infall model for the dust

We have shown that the diffuse infrared emission from dust produced by discrete sources inside the inner region of the Virgo cluster is below any detection capabilities. This situation occurs

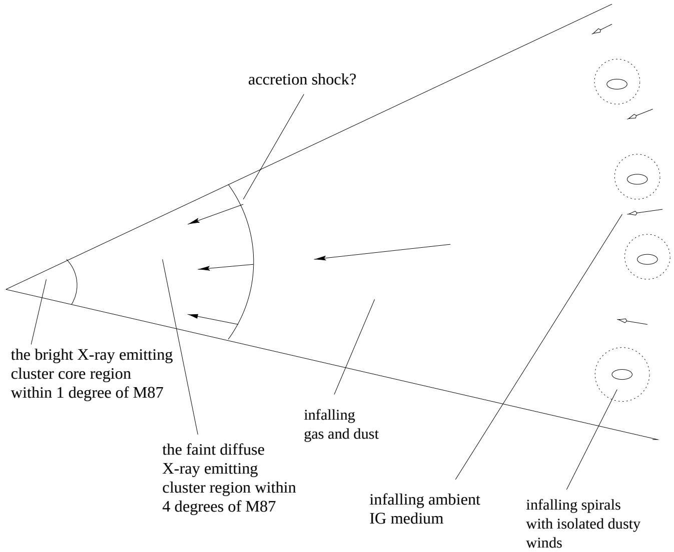

Fig. 5. Schematic view of the infalling of gas and dust into the cluster core

from the fact that there are simply not sufficient strong sources of dust to produce a dust injection rate high enough to replenish the large amount of dust sputtered by the ambient hot plasma. In this section we propose a new mechanism for injecting dust into the ICM, namely dust removed from spiral galaxies by galactic winds throughout their life time, and brought into the cluster by the infalling spirals. This scenario is a corollary of the fact that the clusters are still in the process of forming, by accreting galaxies from the surrounding field environment. The Virgo Cluster is a typical example (and best studied) for such a process. Tully & Shaya (1984) studied the phase space distribution of the spirals in and near the Virgo cluster and developed a mass distribution model in which galaxies within about 8 Mpc of the Virgo cluster are now falling back towards the cluster. Within their model most of the spirals entered the cluster in the last one-third to one-half of the age of the universe. This implies that the Virgo spirals were formed in lower density environments, more like field galaxies and have only lately entered the high-density cluster environment.

Following the idea of clusters accreting from the field, we propose the following scenario (a schematic picture of this infall model is given in Fig. 5.):

1. Spiral galaxies are systematically infalling into the gravitational potential well of the cluster. Following Tully & Shaya (1984) we consider that all the spirals seen today in the Virgo Cluster have entered the cluster in the last 4-6 Gyr at a constant rate. Since the distribution of galaxies in the field is very clumpy, the infalling rate depends on the details of this distribution. But as we do not know the exact distribution of field galaxies over the last 4-6 Gyr, we can only assume a constant rate over this time. Furthermore, if spirals are destroyed or transformed into ellipticals when they approach the cluster core, then there may have been even more spirals infalling into the cluster, than we see today. Thus our assumptions give only a lower limit to the total number of infalling spirals.

2. In addition to the infalling galaxies, there should, presumably, be an accompanying primordial infalling diffuse intergalactic gas component, from which the galaxies originally formed. Little is known about the density and temperature of this intergalactic medium (IGM) in general, but it is believed to have temperatures in the range $10^4 - 10^6$ K. Immediately, prior to galaxy formation one would expect the gas to co-move with the galaxies. At later stages of the infall, gas-gas hydrodynamic interactions may however decouple the gas from the galaxy inflow, and, provided the interactions are gentle enough to avoid heating to virial temperature, would tend to increase the infall rate by removing angular momentum.

3. The diffuse low pressure ambient IGM is favourable to the formation of galactic winds in spirals (Breitschwerdt et al. 1991). If we assume that the galactic winds of spirals were able to inject dust into the IG medium for their full lifetime of 13 Gyr, then large amount of dust is also brought into the cluster.

A basic premise of our analysis is that the spirals infalling into the cluster will be approximately comoving with the (primarily primordial) IG gas and the injected dust and gas from the embedded galaxies. This premise can only be indirectly tested as any infalling IG medium can only be detected once it has been virialised into an X-ray emitting IC medium. Simple analytic models for the growth of clusters are given by Gunn & Gott (1972), in which the infalling baryonic material is relatively cold, such that the hot X-ray emitting IC medium is separated from the infalling gas by a strong accretion shock. In the present work, we tentatively identify the outer boundary of the faint diffuse X-ray emission emission extending $4-5^\circ$ from M87 with a macroscopic accretion shock. The relatively sharp radial cut off of the diffuse X-ray emission shown particularly by the GINGA scan data (Takano et al. 1989) would seem to admit such an interpretation. This allows us to estimate the current upstream density of the infalling IG medium from the observed gas density of $\sim\ 4\times10^{-5}\,\mathrm{cm}^{-3}$ (Schindler et al. 1999; see also Sect. 2) for the boundary of the diffuse X-ray emitting medium. Taking the compression ratio of the accretion shock to be 4, this yields $\mathrm{n_{IGM}}\ \sim\ 10^{-5}\,\mathrm{cm}^{-3}$ for the current number density of the infalling IG medium at a distance of 1.3 Mpc from M87.

We can now use this estimate for $\mathrm{n_{IGM}}$ in conjunction with the observed total mass of baryonic matter emitting X-rays downstream of the accretion shock, which should be made up of infallen matter and the initial perturbation, to test the hypothesis that the infalling galaxies and IG gas are comoving. We can estimate radial infall velocity of the IG gas at the radius of the presumed accretion shock of $\mathrm{R_{shock}} \sim 1.27$ Mpc (4°) from the radial distribution of galaxian velocities derived by Tully & Shaya (1984) in their simple radial infall model (see their Fig. 4). After taking into account the slight differences in the assumed distance to the cluster (16.8 Mpc was derived by Tully & Shaya) we predict the gas infall velocity at the accretion shock to be $\mathrm{v_{infall}}\ \sim\ 800\,\mathrm{km\,s^{-1}}$. From this, we can estimate the current accretion rate of baryonic IG gas, assuming spherical symmetry, as $4\pi\,\mathrm{R^2_{shock}}\,\mathrm{m_H}\,\mathrm{v_{infall}}\,\mathrm{n_{IGM}}\ \sim 3900\,\mathrm{M_\odot\,yr^{-1}}$. Since both the IC medium and the infalling galaxies show marked deviations from spherical symmetry, indicative of the infall of an irregular distribution of clumps, this estimate should be treated as a crude upper limit. Nevertheless, it is remarkable that the 3900 $M_\odot\,yr^{-1}$ multiplied by a presumed age of 1.3×10^{10} yr, or $5.1 \times 10^{13}\,M_\odot$ is close to the $4 \times 10^{13}\,M_\odot$ for the total baryonic gas mass in the (dominant) IC medium component centered on M87 within 1.3 Mpc, as plotted on Fig. 11a of Schindler et al. (1999). (Although Schindler et al. use a hydrostatic model for the derivation of mass from the X-ray emission, we would not expect very different results from a dynamic accretion flow model as the post shock inwards flow velocities are small). This result we use it here to justify our assumption of a radial inflow of relatively cold IG gas, comoving with the galaxies, which provides a medium to sweep grains injected from the embedded spiral galaxies down into the cluster. We also note that the incoming mass flux of the IG medium dominates that of the incoming galaxies, so that it is a safe assumption that the galactic winds themselves should have no significant heating effect on the IG medium.

Here we consider the fate of dust particles ejected in the winds of infalling spiral galaxies. In the following we assume that grains always comove with the ambient gas - i.e. that the grains are charged and the ambient gas is magnetised. There are two main obstacles for such grains reaching the benign environment of the IGM, which is too cool for significant sputtering.

Firstly, the grains have to survive the passage through the hot galactic wind; we will show in the next section that in most cases grains can survive this passage. Secondly, the winds will create local "bubbles" in the ambient IGM, containing wind shocks which provide a further possibility for sputtering. However, the densities are so small that this effect is negligible. According to Castor et al. (1975), the density and temperature in the hot shocked wind region is given by:

$$n_w = 0.01\, n_0^{19/35} (\dot{M}_6\, v_{2000}^2)^{6/35}\, t_6^{-22/35}\, cm^{-3} \quad (14)$$

$$T_w = 1.6 \times 10^6\, n_0^{2/35} (\dot{M}_6\, v_{2000}^2)^{8/35}\, t_6^{-6/35}\, K \quad (15)$$

where

$$\dot{M}_6 = \dot{M}_w/(10^{-6}\, M_\odot\, yr^{-1}),$$
$$v_{2000} = v_w/(2000\, km/s),$$
$$t_6 = t_{gal}/(10^6\, yr),$$

M_w is the mass ejected through the winds during the age of the galaxy t_{gal}, at a constant rate $\dot{M}_w$, v_w is the terminal velocity of the wind, and n_0 is the number density of the ambient IGM. For typical values of $\dot{M}_w = 1\, M_\odot\, yr^{-1}$, $v_w = 500$ km/s (Breitschwerdt et al. 1991) and $n_0 = 10^{-5}\, cm^{-3}$ we obtain $n_w = 4 \times 10^{-7}\, cm^{-3}$ and $T_w = 2.1 \times 10^6$ K. For such a low density the sputtering time of a grain of size 0.1 μm is 2.5×10^{11} yr and therefore this effect can be neglected.

A more fundamental effect is that the bubbles are buoyant, and will tend to rise relative to the cold ambient medium. This effect can potentially impede the inflow of the grains. However, even if the bubbles could grow for a substantial fraction of the Hubble time, it seems very unlikely that the velocity of a boyant bubble relative to the ambient medium could become significant compared to the inflow velocities. A fundamental upper limit for this relative velocity is the sound velocity of the ambient medium, which for T$\sim 10^5$ K is $\sim 33\, km\, s^{-1}$. This is much smaller than the expected escape velocity for a central mass of $2 \times 10^{14}\, M_\odot$ (Schindler et al. 1999), for the scales we consider here (out to 8 Mpc). In particular we note that the Virgocentric infall of the Local Group is 220 km/s (Tammann & Sandage 1985). In practice, as the galaxies approach the inner region of the cluster, they will decouple from the velocity field of the IGM medium. Then it seems unlikely that the bubbles will remain intact, due to the expected relative motions of the galaxies with respect to the primordial IGM. Analogous to stars moving through the ISM of the Milky Way, the bubbles would be expected to develop axi-symmetric "cometary" like structures, in which the hot material can escape into the ambient medium along the trailing axis. We can use the estimate of the density of the baryonic IG medium to check our assumption that sputtering can be neglected for grains released directly into the infalling IGM. Very conservatively, assuming that density varied with redshift as $(1+z)^3$ (i.e. ignoring the comoving density increase due to the infall into the cluster), $n_{IGM} \sim 10^{-5}\, cm^{-3}$ corresponds to 2.7×10^{-4} at z$= 2$, for which (using Eq. (19) and taking the gas temperature to be constant in time at 10^5 K), the sputtering timescale would be less than a Hubble time only for very small grains (of size $\leq 0.002\mu m$). Thus it seems reasonable to suppose that grains can accumulate in the inflowing IG medium since rather early epochs.

In summary, we would expect grains ejected in galactic winds to fall into the cluster, co-moving with the ambient intergalactic gas. In the cold ambient gas outside the X-ray emitting region of the cluster the grains will survive, since there is no mechanism for destruction. But once the gas and grains reach the X-ray region, the grains will be sputtered and collisionally heated, and thus produce infrared emission.

In order to calculate the infrared emission from the intracluster medium, we must first consider destruction processes of grains in the galactic winds, which in principal could reduce the grain injection rate.

5. Grain sputtering and size distribution in the galactic winds

From the study of the parameters of different kind of winds (Breitschwerdt et al. 1991, Breitschwerdt & Schmutzler 1999) we know that the initial conditions in the winds are rather unfavourable to grain survival, due to the high densities and temperatures. Thus the grain survival depends on how rapidly these winds can cool and expand on their way out of the disk. There are mainly two types of galactic winds in the spiral galaxies: winds driven by cosmic rays and thermally driven winds (starburst winds, like in M82). Cosmic ray winds can be classified (Breitschwerdt & Schmutzler 1999) in global winds, that originate from the large-scale expansion of the hot galactic corona, and local winds, which come from individual superbubble regions in the disk. Star-burst winds are stronger, being thermally

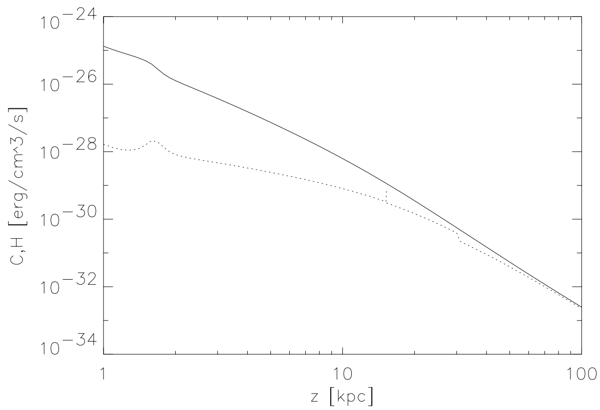

Fig. 6. The cooling rate C (solid line) and the wave damping heating rate H as a function of the distance above the galactic disk d.

driven due to the high gas temperature in their hot interstellar medium.

Here we will consider the parameters of these different kinds of winds, as presented in Breitschwerdt & Schmutzler (1999), who included in their calculations both adiabatic and radiative cooling. Especially for global winds it was shown that the radiative cooling dominates the gas cooling until the temperature drops to a few 10^4 K, when adiabatic cooling becomes important. Again, considering global winds Zirakashvili et al. (1996) have shown that unsaturated non-linear Landau damping may dominate the advection of waves in the plasma and hence lead to local dissipative heating. Up to now there is no self consistent model for galactic winds that includes both the effects of line cooling and heating due to wave damping. Below we argue that the contribution of wave heating is much smaller than that of cooling, and can be neglected. Thus, we have calculated the cooling rate and the heating rate using the solutions for global winds from Breitschwerdt & Schmutzler (1999). The cooling rate C is:

$$\mathrm{C} = \mathrm{n}^2\,\Lambda(\mathrm{T}) \tag{16}$$

where n is the gas density in cm^{-3} and the cooling function $\Lambda(\mathrm{T})$ was taken from Kahn (1976),

$$\Lambda = 1.33 \times 10^{-19}\,\mathrm{T}^{1/2}\ (\mathrm{erg\,cm^3\,s^{-1}}) \tag{17}$$

The upper limit to the heating rate H is:

$$\mathrm{H} = -\mathrm{v_a}\nabla\mathrm{P_c} \tag{18}$$

with $\mathrm{v_a}$ the Alfvén velocity and $\mathrm{P_c}$ the cosmic ray pressure. The effects of heating and cooling can be compared in Fig. 6. Above 1 kpc from the disk, the cooling rate is 3 orders of magnitudes higher, and it is still dominant at 10 kpc. At even higher distances the contribution of the two rates becomes equal, but the gas temperature and density is already below the level where it could produce any efficient dust grain destruction. Therefore we will consider in our calculation the wind solution from Breitschwerdt & Schmutzler (1999).

5.1. Global winds

In the slow global winds that are continuously emitted by the quiescent spiral galaxies, the temperature drops very quickly with the expansion of the wind, and this reduces substantially the grain sputtering. The temperature (T [K]), density (n [cm^{-3}]), and velocity (v [km/s]) profiles above the disk (z[kpc]) are plotted with solid line in Fig. 7, using the data from Breitschwerdt & Schmutzler (1999) (also from D. Breitschwerdt, private communication). The global wind solutions correspond to a flux tube located at a galactocentric distance of 10 kpc, for an adiabatic model whereas an isochoric cooling function was included. These profiles were used for calculating the sputtering time profile, considering the analytical formula from Tsai & Mathews (1995). Thus, the rate at which the radius of the dust grain decreases with time in a hot plasma of temperature T and density $\mathrm{n_H}$ is:

$$\frac{\mathrm{da}}{\mathrm{dt}} = -f\,\mathrm{n_H}\left[\left(\frac{\mathrm{T_d}}{\mathrm{T}}\right)^{2.5} + 1\right]^{-1} \tag{19}$$

Tsai & Mathews showed that this relation is a good approximation to the detailed calculations of Draine & Salpeter (1979) and Tielens et al. (1994), for both graphite and silicate when $f = 3.2 \times 10^{-18}\mathrm{cm^4\,s^{-1}}$, and $\mathrm{T_d} = 2 \times 10^6$ K. The sputtering time can be then computed as:

$$\mathrm{t_{sput}} = \mathrm{a}\left|\frac{\mathrm{da}}{\mathrm{dt}}\right|^{-1} \tag{20}$$

which for gas temperatures $10^6 < \mathrm{T} < 10^9$ K reduces to the formula (5). In Fig. 7 we show the sputtering time for a big grain of radius $\mathrm{a} = 0.25\,\mu$m. $\mathrm{t_{sput}}$ increases rapidly to more than 10^{10} yr, but smaller grains have shorter survival times. The minimum grain size that can survive in the wind is derived from the cumulative size loss Δa, which is obtained by integrating the sputtering rate over the time it takes the wind to go out the galaxy:

$$\Delta\mathrm{a} = \int \frac{\mathrm{da}}{\mathrm{dt}}\mathrm{dt} \tag{21}$$

The cumulative size loss Δa is plotted in Fig. 8 (solid line), and from the saturation value we derive a minimum grain size that survives sputtering $\mathrm{a_{surv}} = 0.0071\,\mu$m.

We assume that the initial size distribution in the wind is given again by a power law of index k=3.5. The sputtering modifies the size distribution, in the sense that grains smaller than $\mathrm{a_{surv}}$ will be completely destroyed while bigger grains will end with a final size $\mathrm{a} - \mathrm{a_{surv}}$. The final size distribution will be given by:

$$\mathrm{N(a)} \sim (\mathrm{a} + \mathrm{a_{surv}})^{-k} \tag{22}$$

In the case of global winds grains as small as $0.0072\,\mu$m can survive, which means that the grain size distribution is only negligible changed, and most of the dust will be injected in the IC medium.

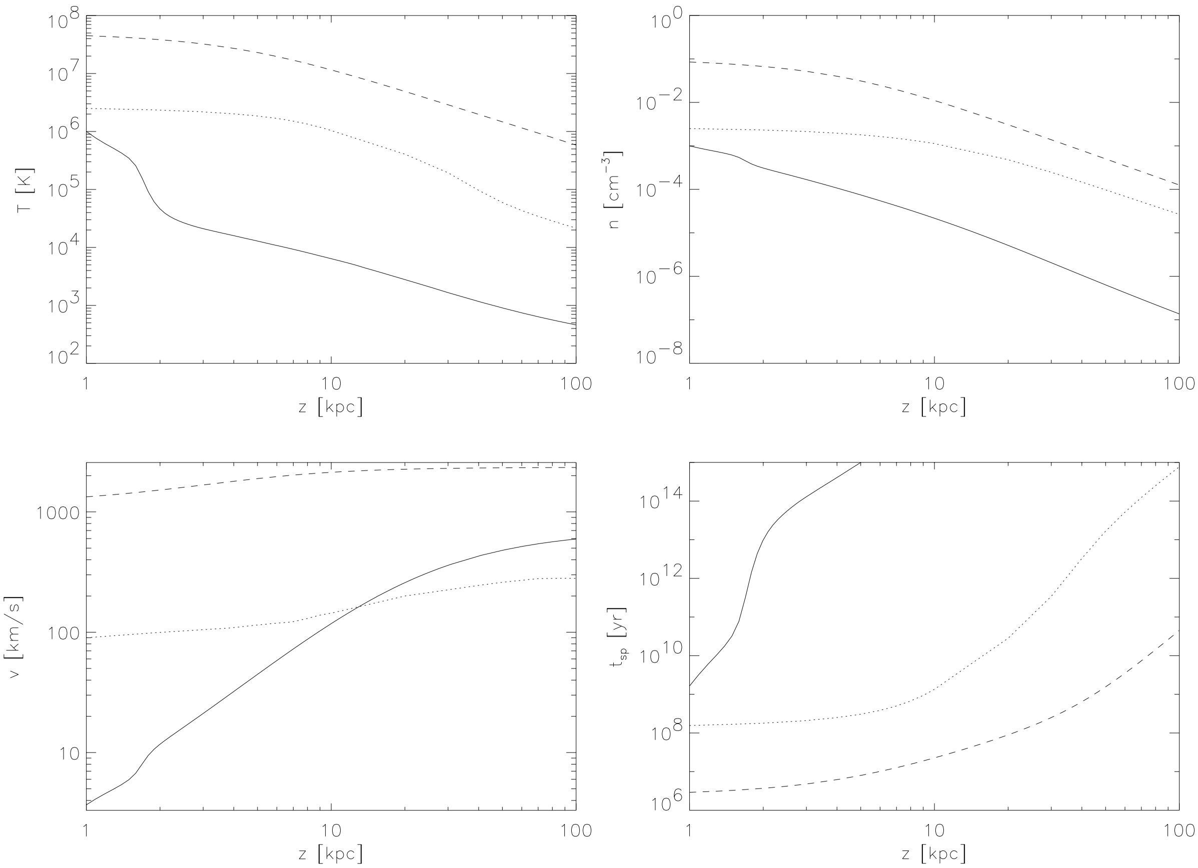

Fig. 7. The parameters of galactic winds: temperature T, density n, and velocity v as a function of the distance above the galactic plane, z. The sputtering time t_{sput} for a grain size of radius $a = 0.25\,\mu$m is also plotted in the lower-right panel. The global winds are plotted with solid line, the local winds with short-dashed line, and the star-burst winds with long-dashed line.

5.2. *Local winds*

Local winds have initially higher densities and temperatures, and these quantities remain almost constant till the wind reaches 10 kpc above the galactic disk (Breitschwerdt & Schmutzler 1999). The corresponding temperature, density and velocity profiles are plotted in Fig. 7 with short-dashed lines. We expect that less grains will survive the wind. Following the same recipe like in the case of global winds we obtain a minimum grain size that survives, $a_{surv} = 0.084\,\mu$m. This is higher than the minimum grain size that survives the global winds, but still a substantial amount of grains will survive. The corresponding sputtering time and cumulative size loss Δa are plotted with short-dashed lines in Fig. 7 and 8, respectively.

5.3. *Star-burst winds*

The very energetic starburst winds can be traced already from 0.1 kpc above the disk, but in Fig. 7 and 8 we plot (long-dashed lines) only the range between 1 and 100 kpc, in order to have the same range as for the other two type of winds. The temperature and density is more than one order of magnitude higher than for global winds, and even at 10 kpc these parameters are still high enough to sputter quite efficiently the dust grains. Despite the fact that the wind velocity is also very high, the minimum grain size that survives is $\Delta a = 0.3\,\mu$m. But such big grains are rare in the diffuse interstellar medium. We conclude that star-burst winds are not able to inject dust into the IC medium.

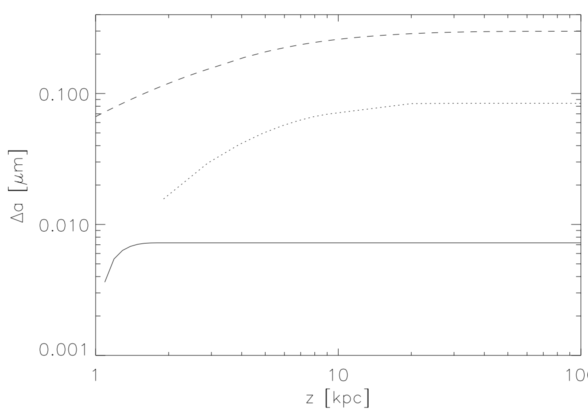

Fig. 8. The cumulative size loss Δa for different galactic winds, as a function of the distance above the galactic plane, z. The global winds are plotted with solid line, the local winds with short-dashed line, and the star-burst winds with long-dashed line. The saturation value for each distribution gives the minimum grain size that survives the wind.

6. The emission spectrum produced by dust falling into the cluster core

We have seen that dust grains survive mainly in global winds, and that their size distribution is not significantly changed by sputtering in the injection process. If the initial dust-to-gas ratio in the wind is $Z_d = 0.0075$ (the Galactic value), the grains will be injected into the IG medium with $Z_d = 0.0071$ after sputtering, which means that the dust-to-gas ratio is practically unchanged. The mass loss rate through global galactic winds is of the order of $1\,M_\odot/yr$ for a galaxy like the Milky Way (Breitschwerdt et al. 1991, Zirakashvili et al. 1996). The local winds can also inject grains into the IC medium, but with a smaller dust-to gas ratio, and with a modified size distribution given by (22). Furthermore, the mass loss rate from these winds is one order of magnitude lower than for the global winds (Breitschwerdt & Schmutzler 1999). And local winds do not happen continuously over the life time of the spirals, but rather in episodes that are connected with the life time of their parent giant HII region superbubbles. Thus we neglect their contribution. Star-burst winds can inject large amounts of gas in the IC medium, even more than $10\,M_\odot$/yr, but the injected gas is depleted of grains. To conclude, spiral galaxies release grains in the IC medium mainly through global galactic winds.

6.1. Injection rate of grains into the intracluster medium

We estimate the total infalling rate of grains into the cluster by scaling the mass loss rate in galactic winds to the blue luminosity of infalling spirals. Following Tully & Shaya (1984) (see Sect. 4) let us suppose that all galaxies currently seen within 6° of M87 arrived at a constant rate within the last 5 Gyr.[1] These observed spirals have a total blue luminosity of $7.15 \times 10^{11}\,L_\odot$ (Binggeli et al. 1987), so that we can express the infalling rate of luminosity as $1.43{\times}10^{11}\,L_\odot\,Gyr^{-1}$. We further assume that the galactic winds were able to inject dust into the IG medium for their full lifetime of 13 Gyr. Then, scaling to the wind injection rate of $1\,M_\odot\,yr^{-1}$ for the Milky Way ($L_B \sim 1.6 \times 10^{10}\,L_\odot$; de Vaucouleurs & Pence 1978) as estimated by Breitschwerdt et al. (1991), each $1.6{\times}10^{10}\,L_\odot$ entering the cluster will bring with it an accumulated wind-ejected gas mass of $13{\times}10^9\,M_\odot$. These estimates then lead to a gas infall rate from galactic winds of $116\,M_\odot\,yr^{-1}$. To calculate the corresponding grain infall rate we take the dust-to-gas mass ratio in the ejected winds, averaged over the 13 Gyr, to be the solar value of 0.0075 to yield a dust injection rate of $0.87\,M_\odot\,yr^{-1}$. This may be quite conservative, bearing in mind that the abundances of the galactic winds should be strongly enhanced compared to the ambient interstellar medium (Völk 1991).

In addition to dust injected into the external IGM by galaxies infalling for the first time, there may also be a secondary contribution from spirals which entered the hot IC medium at previous epochs, but have orbits taking them back beyond the accretion shock, where they can again inject dust.[2] The maximum time since the currently seen spirals entered the cluster ($\sim$5 Gyr) is not much longer than the $\sim$3.2 Gyr needed to traverse the volume enclose by the accretion shock on a radial path. Thus, only some fraction - perhaps one third - of the spirals will have passed back through the accretion shock. Their residence times after re-entry depends on the actual orbits and are thus very uncertain, but may be of the order of 2 Gyr, in any case much less than the $\sim$13 Gyr for the freshly infalling objects. If one third of the galaxies contribute grains to the inflow for 2 Gyr after reentry, the gas and dust injection rates calculated above (for the freshly infalling systems) should be augmented by $\sim$5 percent to 122 and $0.91\,M_\odot\,yr^{-1}$ respectively.

Finally, to calculate the dust injection rate into the IC medium, we should take account of the fact that the accretion shock is not stationary, but advancing outwards in the cluster reference frame at some low speed v_{adv}. Thus the true injection rate of grains into the hot IC medium will be somewhat greater than that given by the infall rate (as calculated above) by a factor $\zeta = (v_{adv}+v_{infall})/v_{infall}$. A rigorous calculation of ζ is beyond the scope of this paper, but an upper limit - for the case that the accretion shock had a compression ratio of 4 and the material downstream of the accretion shock was almost stationary in the cluster reference frame - would be 1.33.[3] Another estimate for ζ can be obtained from the estimate of $v_{infall} \sim 800\,km\,s^{-1}$ from the infall of the galaxies (following Tully & Shaya (1984) - see Sect. 4) and a crude value for v_{adv} of $\sim 800\,km\,s^{-1}$ which is the accretion shock radius (1.27 Mpc) divided by the age of the cluster (13 Gyr). This yields $\zeta \le 1.125$. We will assume $\zeta = 1.1$, from which we obtain final estimates of 134 and $1.0\,M_\odot\,yr^{-1}$ for the gas and dust injection rates into the IC medium.

6.2. Heating and sputtering of injected grains

In order to calculate the heating of grains injected from the inflowing IG medium we recall consider the X-ray morphology of the Virgo Cluster, as summarised in Sect. 2. We only consider the dominant M87 subcluster, which accounts for 71% of the total emission out to 4-5°. This consists of the dense hot X-ray core region extending 1° around M87, and the faint diffuse emission extending 4-5° from M87, which produces 15% of the total X-ray flux (Böhringer et al. 1994). We have identified the boundary of the faint diffuse emission as an accretion shock (Sect. 4).

Grains injected at the supposed accretion shock should be heated by a plasma of density $\sim 4{\times}10^{-5}\,cm^{-3}$ and temperature $\sim 3 \times 10^7$K. The sputtering timescales in this most tenuous region of the IC medium are $2.5{\times}10^9$ yr of grains of size 0.1 μm. Although comparable to the infall time for galaxies from the accretion shock radius to the centre, this sputtering timescale

[1] We note that this may actually yield a lower rate than the actual rate if some fraction of the infalling spirals had been transformed into ellipticals in this time.

[2] We assume winds are suppressed while the galaxies are in the pressurised IC medium.

[3] In reality the downstream flow clearly has to have some inwards velocity to maintain pressure equilibrium against gravity in the IC medium.

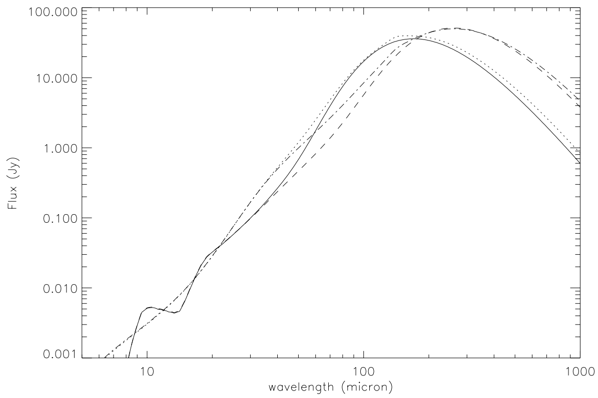

Fig. 9. The infrared spectrum produced by dust infalling into the cluster core, in two extreme cases: the grains are mainly heated by the diffuse X-ray plasma inside the 4° radius region (dashed-line for silicate grains and dashed-dotted lines for graphites); the grains are heated when they enter the dense 1° core region of the Virgo cluster (solid line for silicate grains and dotted lines for graphite grains).

does not mean that the IR emission will be distributed over a broad range of radii. The grains will follow the inflow of the gas downstream of the accretion shock, which should be actually quasi hydrostatic. Thus, in this simple homogeneous picture for the cluster the grains would be expected to be heated and sputtered in the vicinity of the accretion shock 4-5 degrees from the cluster core, and the infrared emission would trace the morphology of the accretion shock surface. In this scenario, the grain heating will be relatively low as the grains never reach the denser core regions of the IC medium, and the emission will predominantly arise in the submillimetre range. We refer to this as case A.

In reality the structure of the M87 subcluster is much more irregular than this simple representation. Böhringer et al. (1994) have shown that in the western part of the cluster the X-ray emission falls off more steeply, while the northern edge of the cluster is less well defined, with the cluster boundary dissolving into several individual subclumps. Because of the uncertainties in the 3D structure of the cluster, it is very difficult to predict the actual fate of infalling grains reaching the accretion shock radius. In particular, the accretion may be fundamentally clumpy in nature, with infalling clumps of dust-bearing gas reaching different depths before interacting and merging with an irregularly shaped intracluster medium. In this scenario it may be possible for clumps infalling through certain position angles to directly interact with the dense X-ray core region extended 1° around M87. Then the grain heating will be stronger, with most radiation being produced in the FIR. We refer to this as case B.

We note that the instantaneous luminosity will be very similar which ever of case A and B is nearer the truth, provided the grain injection rate is constant over the sputtering timescale. For a steady state between injection and destruction, the effect of the increased heating expected for grains reaching the central dense regions of the IC medium (Case B) will almost exactly be balanced by the shorter grain survival times, since sputtering timescales are only weakly dependent on temperature for plasma hotter than $\sim 10^6$ K.

Table 4. The characteristics of the infrared spectrum in two extreme cases (A and B), both for silicate and graphite grains. The table lists the wavelength corresponding to the maximum emission, the colour of the spectrum and fluxes.

	Case A ($r = 4°$)			Case B ($r = 1°$)		
	λ_{max} [μm]	$\frac{F259}{F175}$	F_{259} [Jy]	λ_{max} [μm]	$\frac{F175}{F100}$	F_{175} [Jy]
Si	259	1.4	51.3	172	2.1	35.9
Gra	259	1.3	50.0	163	2.2	39.4

The spectrum of the submillimeter emission in case A is given in Fig. 9, both for silicate grains (dashed line) and for graphite grains (dashed-dotted line). In the calculation we assume a steady-state solution for the balance between dust destruction and injection just downstream of the accretion shock, following the procedure described in Sect. 2. The peak of the emission, the colour of the spectrum and the fluxes are given in Table 4. Fig. 9 also shows the predicted emission from case B (solid line for silicates and dotted line for graphites). Here the spectrum was calculated under the assumption that the grains will survive and emit only in the outer spherical shell of the central core of cluster at radii of $\sim 1°$ ($n_e = 0.0007\,\mathrm{cm}^{-3}$, $T_e = 3.37 \times 10^7$, see Table 1). The parameters of this emission are also given in Table 4.

7. Discussion

We have calculated the infrared emission for the Virgo cluster taking into account all possible sources of dust inside the cluster core. We have shown that there are not enough discrete sources of dust in the Virgo cluster to produce detectable diffuse emission. This is compounded by the fact that galaxian sources of dust embedded in the IC medium will certainly not be able to provide a smooth distribution of grains within the volume of the IC medium as sputtering timescales are invariably shorter than transport timescales over a typical separation between galaxies. Of all potential discrete sources only the stars could be thought of as giving rise to a smooth emission component, though, for the Virgo cluster, this will only amount to 20 percent of the emission from the infalling intergalactic grains. Thus, any detection of truly diffuse FIR emission is likely not to trace dust injected by galaxies inside the cluster core, but rather the inflow of grains to the cluster from the external intergalactic medium. Since younger clusters, like the Virgo cluster still have spiral galaxies infalling into the cluster, we might expect them to have a larger amount of infalling dust, and thus a higher FIR emission. Thus, in general, the phenomenon of diffuse intracluster FIR emission may give information on the current dynamic age of the cluster. In this sense it is complementary to the measurements of X-ray emission which broadly relate to all the baryonic matter accumulated over the lifetime of the cluster.

7.1. Detectability and recognition of IC dust emission

Our estimates for the IR emission rely on a chain of quite poorly determined quantities, such as the dependence of mass ejection in galactic winds on blue luminosity, uncertainties in the dynamical properties of the inflow, and the metallicity of the wind ejected material. Detection of diffuse IR emission may be useful to constrain some of these factors. On the basis of the simple estimates given in Table 4, however, it will be fundamentally difficult to detect such emission from nearby clusters. The high angular sizes will lead to severe confusion of the IC IR emission with foreground emission, which will be difficult to alleviate with multiwavelength studies given that the predicted emission has quite similar colours to the galactic cirrus. The best possibility for detection is for our case B scenario in which the cluster is fundamentally clumpy, as then the emission may be concentrated over smaller solid angles (scales of 1° as opposed to 4° for the case A scenario). In general, because the grain sputtering timescales are shorter than the grain transport timescales, once the grains have reached their sputtering/injection sites, they will in general trace surfaces of injection rather then be distributed over a depth of volume. This may lead to some limb-brightening effects which could aid detection, though care would have to be taken to distinguish these structures from the trails predicted from spiral galaxies undergoing ram-pressure stripping discussed in Sect. 3.3.

It is more likely that diffuse intracluster emission could be detected towards distant clusters of lower angular size. Referring again to our illustrative scenarios of grains being sputtered in the diffuse X-ray emitting plasma (Case A) or when they first enter the 1 degree core region of the cluster (Case B), we address the question of how the Virgo cluster would appear if situated at a cosmological distance of z=0.5. The 4 degree region of the cluster would be seen as a source of $3'$. So the cluster will look like a compact source, and to detect this source we need to have only enough total flux. If we consider a Euclidian flat geometry with q_0=1/2 we obtain a flux of 1.5 mJy (redshifted at $\lambda = 389\,\mu$m) for Case A or a flux of 1 mJy (redshifted at $\lambda = 263\,\mu$m) for Case B. There will be of course the emission from dust within the cluster galaxies. Here, the main confusion problem would be with the FIR emission from constituent spiral galaxies. To estimate the galaxy contribution to the total FIR emission we used the correlation of the B magnitude of 105 disk galaxies selected from the Virgo Cluster Catalogue with their IRAS 100 micron emission. We found $\mathrm{S}_{\nu}(100\mu m) \sim \mathrm{S}_{\nu}(\mathrm{B})^{1.25}$ in mJy. Using again a King profile for the Virgo Cluster spiral galaxies we derived a total blue luminosity within the 4 degrees region from the cluster centre of $\mathrm{L_B} = 3.7 \times 10^{11}\,\mathrm{L}_{\odot}$. This translates into a flux of 295 Jy at 100 micron. For a colour $\mathrm{F}_{175}/\mathrm{F}_{100} = 1.5$ we estimate that the cluster galaxies should contribute with 442 Jy to the total flux at 160 μm. This translates into a flux of 13 mJy for a redshifted cluster, which is still one order of magnitude higher than the intracluster emission. Thus, a combination of good surface brightness performance and resolution will be required for a unambiguous detection of IC dust emission. Especially as the emission peaks in the submillimeter, this type of observation will be particularly well suited to the new generation of submillimeter interferometers.

Finally, we remark that galaxies may not be the only sources of IG grains, especially in the early universe. FIR/ sub-mm observations of clusters may in general provide new information of the abundance of the IG grains, which is currently only poorly constrained.

7.2. The optical extinction in clusters

From our infalling model it is obvious that the extinction in clusters will be dominated by dust upstream the accretion shock. If we suppose that grains are uniformly distributed within the volume of the cluster, we obtain an $\mathrm{A_B} = 0.005$ magnitudes at a distance 4 degrees from the cluster center. However, this extinction could increase when some limb brightness effects are taken into account. Furthermore, extinction may be higher on some optical paths if we allow for clumpy accretion of infallen material. In passing we mention that these calculations are obtained under our very conservative assumption that galactic winds have the Galactic gas-to-dust ratio. As discussed in Sect. 6.1, the abundance of galactic winds may be strongly enhanced as compared to the ambient interstellar medium (Völk 1991) and thus much more dust can then be injected in the IG medium. Thus the amount of extinction may be sensitive to the assumed accretion rate of dust and to the geometrical effects in the cluster. Our predicted extinction should be compared to the few tenths of optical depth predicted by some optical studies which found a deficit of distant galaxies (Zwicky 1962; Karachentsev & Lipovetskii 1969; Bogart & Wagoner 1973; Szalay et al. 1989) or quasars (Boyle et al. 1988; Romani & Maoz 1992). However there are also some optical studies that do not support the presence of extinction in clusters. Maoz (1995) found out that radio-selected quasars behind Abell clusters are not redder than quasars that do not have a cluster in foreground. He also suggested that previous results that claimed the avoidance of foreground Abell clusters by optically selected quasars can be explained as being due to selection effects. Ferguson (1993) studied the colour versus $\mathrm{Mg_2}$ relation for elliptical galaxies in cluster, group and field samples. He also found no evidence for excess reddening in clusters or groups.

7.3. Relation to other observables

Our predictions for diffuse FIR/sub-mm intracluster emission rely on the ubiquitous existence of "global" winds from quiescent spiral galaxies, enriching the infalling intergalactic medium with metals, partly as dust grains. As noted by Völk (1991), it should be expected that the metallicity of the ejected wind material should be substantially higher than for the interstellar medium of the disks, which has consequences for the chemical evolution of spirals. An interesting corollary, therefore, of any detection of diffuse IR emission in the periphery of the cluster, is the implication for the environmental effects on the chemical evolution of spiral galaxies. There is some evidence (Skillman et al. 1996) that spiral galaxies in the core region of the Virgo cluster have enhanced metallicities compared to counterparts in the cluster periphery and field environment. Skillman et al. (1996) account for this abundance contrast in terms of scenarios invoking the accretion of metal-poor cold intergalactic material to dilute the abundances of field galaxies, by supposing that the accretion is suppressed for galaxies in the cluster core due to the hot environment. We propose the opposite scenario to explain the abundance contrast between field and cluster, namely the ejection of overabundant interstellar material in quiescent winds of field galaxies, as opposed to the cluster core, where quiescent winds are predicted to be suppressed by the high pressure environment. We note that a wind scenario for chemical abundance regulation would require a larger integrated nucleosynthetic production over the lifetime of a galaxy as compared to a regulation by accretion, due to the loss of a substantial amount of metals to the IG medium.

The infall scenario may also alleviate the problem of explaining the absolute metal content of the intracluster medium purely in terms of the nucleosynthetic history of galaxies, principally ellipticals (e.g. Okazaki et al. 1993) embedded in the IC medium, as some proportion of the metals will then have been injected through the winds of spirals embedded in the infalling IG medium. Recently, Wiebe et al. (1999) also considered the possibility that galactic winds from spiral galaxies contribute to the chemical enrichment of the ICM, though they did not take into account the fact that winds are suppressed in the dense ICM by the high pressure environment. In our infall model, one possible observational manifestation would be the expected X-ray emission in the periphery region of the cluster, just downstream of the accretion shock. Once sputtered, the grains will release refractory elements into the gas phase, which will radiate line emission to supplement emission from the directly injected non-refractory component. The radial profiles of line emission may give some indication of the infall history of these metals.

Our predictions for the origins of diffuse infrared emission in the IC medium may also have a physical corollary to the observational situation regarding the diffuse synchrotron emission. Grains are short-lived and cannot move far from their sources. But by the same token, relativistic electron cannot move far from their sources due to inverse Compton and synchrotron losses. It is tempting to imagine a scenario in which both phenomena are localised around an accretion shock and would be interesting to compare the morphology of diffuse IR and radio emission from this viewpoint. The possibility of particle acceleration at the location of extended accretion shocks around the clusters has been recently discussed by Enßlin et al. (1998). They identified the so called cluster radio relics to be powered by the accretion shock produced by the large-scale gas motion around the clusters.

Finally, we can examine whether submillimeter emission from intracluster dust, as predicted here, might be detectable in experiments to detect Sunyaev-Zeldovich (SZ) excess towards clusters. At increasing redshifts, the wavelength of peak emission from the IC dust may move close to the SZ peak around $\lambda = 0.8$ mm. The appearance of both the intracluster dust emission and the SZ excess is predicted to be related to the morphology of the diffuse X-ray Bremsstrahlung from the ICM. To get

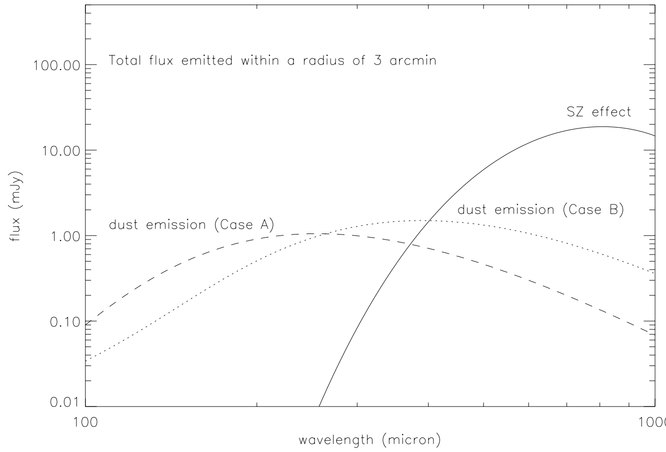

Fig. 10. Predicted flux emitted within a radius of 3 arcmin by a cluster like Virgo Cluster, at a redshift z=0.5. With solid line we plot the thermal SZ effect, with dashed line the dust emission for Case A and with dotted line the dust emission as estimated for Case B.

an estimate for the relative emissions from the two phenomena we have estimated the (thermal) SZ effect that we would observe for a cluster like the Virgo Cluster, using the parameters for the 4 degree central region of Virgo, but with the cluster redshifted to z=0.5. The Comptonization parameter y (see Rephaeli 1995) was calculated by integrating the gas density profile of the cluster (Schindler et al. 1999) for a constant temperature $\mathrm{T} = 3.3 \times 10^7$ K. We obtained an averaged $\mathrm{y} = 4.3 \times 10^{-6}$, which is consistent with the upper limit determined from the COBE/FIRAS database, $\mathrm{y} \leq 2.5 \times 10^{-5}$ (Mather et al. 1994). The corresponding temperature change due to the scattering was calculated in the non-relativistic case (Rephaeli 1995):

$$\Delta T_{\rm nr} = \left[\frac{x\,(e^x+1)}{e^x-1} - 4\right] \mathrm{T_0\,y} \qquad (23)$$

where x=hν/kT is the nondimensional frequency, T is the radiation temperature and $\mathrm{T_0} = 2.726$ (as determined by the COBE/FIRAS; Mather et al. 1994). The corresponding surface brightness due to this change in temperature was multiplied with a solid angle of $3'$ radius (as seen for the 4 degrees inner region of the Virgo Cluster at a redshift z=0.5) and the integrated flux is shown in Fig. 10. The fluxes estimated for the diffuse dust emission (in both Case A and Case B) for the Virgo Cluster (redshifted to z=0.5) are also plotted for comparison in Fig. 10. It is obvious that for wavelengths less than 400 micron the diffuse emission is dominated by dust emission. At longer wavelengths the dust emission becomes less important, reaching about 5 percent of the S-Z emission at the S-Z peak. However, these considerations relate to the integrated fluxes. If the diffuse dust emission could be spatially resolved, as indeed it must be to distinguish it from emission from discrete sources in the cluster, it may be possible to distinguish it from the SZ emission due to it's predicted limb brightening at the boundary of the accretion shock. Indeed, in the outermost regions of the cluster, IC dust emission may give a significant signal compared to the smoothly, centrally peaked SZ emission.

8. Summary

In this work we show that any detection of a diffuse FIR intracluster emission is likely not to trace dust injected by galaxies inside the cluster core, since there are not enough discrete sources of dust to produce detectable emission. We propose that the diffuse intracluster FIR emission may trace the current accretion rate of the cluster, which give information on the current dynamic age of the cluster. Even in this case the estimated amount of dust in the cluster is lower than suggested in earlier work (Dwek et al. 1990). The main results of this paper are listed below:

- The infrared emission from dust injected by intergalactic stars inside the core region of the Virgo cluster is a factor of ~ 10 below the detection limit of currently available telescopes.
- The amount of intracluster infrared emission produced by dust ejected by early type galaxies in the inner core of Virgo cluster is negligible even in the upper limit calculation.
- The IR emission coming from dust stripped from late-type galaxies is localised and connected to the parent galaxy, and does not account for a diffuse intracluster IR component.
- For dynamically young clusters like the Virgo cluster we propose a new mechanism for injecting dust in the ICM, namely dust removed from spiral galaxies by galactic winds throughout their life time, and brought into the cluster by the IGM. A basic premise of this scenario is that the spirals infalling into the cluster comove with their ambient IG medium and the injected dust and gas from the embedded spirals.
- In this work we identify the outer boundary of the diffuse X-ray emission of the Virgo Cluster, extending $4-5°$ from M87, with a macroscopic accretion shock. In a simple homogeneous picture for the cluster the infalling grains would trace the morphology of the accretion shock surface. Since the density of the ambient plasma is low in this region, the heating is relatively low and the infrared emission arise in the submillimetre range. If the accretion is fundamentally clumpy in nature, it is possible for clumps infalling through certain position angles to directly interact with the dense X-ray core region of the cluster. Then the infrared emission is shifted to shorter wavelengths.
- For nearby clusters it will be fundamentally difficult to detect infrared emission from intracluster dust, due the large volumes considered and to the relative low masses of dust. It is more likely that diffuse intracluster emission could be detected for distant clusters. Because the cluster emission is dominated by emission from cluster member galaxies, any detection of a diffuse component requires a combination of good surface brightness performance and resolution. This type of observation would be well suited to the new generation of submillimeter interferometers.

Acknowledgements. We would like to thank Dr. M. Voit for the careful refereeing of the manuscript. We gratefully acknowledge Dr. D. Breitschwerdt for providing us with his calculated data on galactic winds. We also kindly acknowledge Dr. U. Fritze-von Alvensleben for providing us with the HRD population model needed in Sect. 3.1. We would like to thank Drs. A. Burkert and A. Blanchard for interesting discussions.

References

Allen C.W., 1973, Astrophysical Quantities, third edn. Athlone, London
Arimoto N., Yoshii Y., 1987, A&A 173, 23
Arnaud K.A., Mushotzky R.F., 1998, ApJ 501, 119
Bahcall J.N., Flynn C., Gould A., 1992, ApJ 389, 234
Balsara D., Livio M., O'Dea C.P., 1994, ApJ 437, 83
Binggeli B., Sandage A., Tammann G.A., 1985, AJ 90, 1681
Binggeli B., Tammann G.A., Sandage A., 1987, AJ 94, 251
Binggeli B., Popescu C.C., Tammann G.A., 1993, A&AS 98, 275
Bogart R.S., Wagoner R.V., 1973, ApJ 181, 609
Böhringer H., Briel U.G., Schwarz R.A., et al., 1994, Nature 368, 828
Boyle B.J., Fong R., Shanks T., 1988, MNRAS 231, 897
Breitschwerdt D., Schmutzler T., 1999, A&A 347, 650
Breitschwerdt D., McKenzie J.F., Völk H.J., 1991, A&A 245, 79
Castor J., McCray R., Weaver R., 1975, ApJ 200, L107
David L.P., Forman W., Jones C, 1990, ApJ 359, 29
David L.P., Forman W., Jones C, 1991a, ApJ 369, 121
David L.P., Forman W., Jones C, 1991b, ApJ 380, 39
de Vaucouleurs G., Pence W.D., 1978, AJ 83, 1163
Dickey J.M., Lockman F.J., 1990, ARA&A 28, 215
Draine B.T., Anderson N., 1985, ApJ 292, 494
Draine B.T., Salpeter E.E., 1979, ApJ 231, 77
Dressler A., 1980, ApJ 236, 351
Dwek E., 1986, ApJ 302, 363
Dwek E., 1987, ApJ 322, 812
Dwek E., Arendt R.G., 1992, ARA&A 30, 11
Dwek E., Smith R.K., 1996, ApJ 459, 686
Dwek E., Werner M.W., 1981, ApJ 248, 138
Dwek E., Rephaeli Y., Mather J.C., 1990, ApJ 350, 104
Enßlin T.A., Biermann P.L., Klein U., Kohle, S., 1998, A&A 332, 395
Ferguson H.C., 1993, MNRAS 263, 343
Ferguson H.C., Tanvir N.R., von Hippel T., 1998, Nature 391, 461
Gail H.-P., Sedlmayr E., 1975, A&A 43, 17
Gehrz R.D., 1989, in Interstellar Dust, ed. L.J. Allamandola, A.G.G.M. Tielens (Kluwer Academic Publishers), p. 445
Giovanelli R., Haynes M., 1983, AJ 88, 881
Guhathakurta P., Draine B.T., 1989, ApJ 345, 230
Gunn J.E., Gott J.R., 1972, ApJ 176, 1
Haynes M., Giovanelli R., 1986, ApJ 306, 466
Jones A.P., Tielens A.G.G.M., Hollenbach D.J., McKee C.F., 1997, in Astrophysical Implications of the Laboratory Study of Presolar Materials, ed. T.J. Bernatowicz, E.K. Zinner (AIP Conference Proceedings 402), p. 595
Kahn F.D., 1976, A&A 50, 145
Karachentsev I.D., Lipovetskii V.A., 1969, Soviet Phys. 12, 909
Koyama K., Takano S., Tawara Y., 1991, Nature 350, 135
Laor A., Draine B.T., 1993, ApJ 402, 441
Leger A., Jura M., Omont A., 1985, A&A 144, 147
Maoz D., 1995, ApJ 455, L115
Mather J., Cheng E.S., Cottingham D.A., et al., 1994, ApJ 420, 439
Mathis J.S., Rumpl W., Nordsieck K.H., 1977, ApJ 217, 425
Matsumoto H., Koyama K., Awaki H., et al., 1996, PASJ 48, 201
Matteucci F., Tornambe A., 1987, A&A 185, 51
Moore B., Katz N., Dressler A., Oemler A.J., 1996, Nature 379, 613
Nulsen P.E.J., Böhringer H., 1995, MNRAS 274, 1093

Okazaki T., Chiba M., Kumai Y., Fujimoto M., 1993, PASJ 45, 669
Quillen A.C., Rieke G.H., Rieke M.J., Caldwell N., Engelbracht C., 1999, ApJ 518, 632
Rangarajan D.A., White D.A., Fabian A.C., 1995, MNRAS 277, 1047
Rephaeli Y., 1995, ARA&A 33, 541
Roberts M.S., Haynes M.P., 1994, ARA&A 32, 115
Romani R.W., Maoz D., 1992, ApJ 386, 36
Schindler S., Binggeli B., Böhringer, H., 1999, A&A 343, 420
Skillman E.D., Kennicutt R.C., Shields G.A., Zaritsky D., 1996, ApJ 462, 147
Stickel M., Lemke D., Mattila K., Haikala L.K., Haas M., 1998, A&A 329, 55
Szalay A.S., Hollósi J., Tóth G., 1989, ApJ 339, L5
Takano S., Awaki H., Koyama K., et al., 1989, Nature 340, 289
Tammann G.A., Sandage A., 1985, ApJ 294, 230
Tielens A.G.G.M., McKee C.F., Seab C.G., Hollenbach D.J., 1994, ApJ 431, 321
Tsai J.C., Mathews W.G., 1995, ApJ 448, 84
Tsai J.C., Mathews W.G., 1996, ApJ 468, 571
Tully R.B., Shaya E.J., 1984, ApJ 281, 31
Voit G.M., Donahue M., 1995, ApJ 452, 164
Völk H.J., 1991, in Proc. IAU Symp. 144, "The interstellar disk-halo connection in galaxies", ed. H. Bloemen, p. 345
Whittet D.C.B., 1992, in "Dust in the Galactic Environment"(Institute of Physics Publishing), eds. R.J. Tayler, R.E. White, p. 213
Wiebe D.S., Shustov B.M., Tutukov A.V., 1999, A&A 345, 93
Wise M.W., O'Connell R.W., Bregman J.N., Roberts M.S., 1993, ApJ 405, 94
Young J.S., Scoville N.Z., 1991, ARA&A 29, 581
Zirakashvili V.N., Breitschwerdt D., Ptuskin V.S., Völk H.J., 1996, A&A 311, 113
Zwicky F., 1962, in Problems of Extragalactic Research, ed. G.C. McVittie (New York: Macmillan), p. 149